Available online at www.sciencedirect.com
ScienceDirect
Journal of the European Ceramic Society 31 (2011) 3095–3101
www.elsevier.com/locate/jeurceramsoc

Conductivity and electrochemical performance of $(Ba_{0.5}Sr_{0.5})_{0.8}La_{0.2}Fe_{1-x}Mn_xO_{3-\delta}$ cathode prepared by the citrate–EDTA complexing method

I-Ming Hung [a,*], Chun-Jing Ciou [a], Yi-Jia Zeng [a], Jun-Sheng Wu [a], Yu-Chen Lee [a], Ay Su [b], Shih-Hung Chan [b]

[a] *Yuan Ze Fuel Cell Center, Department of Chemical Engineering and Materials Science, Yuan Ze University, No. 135, Yuan-Tung Road, Chungli, Taoyuan 320, Taiwan*

[b] *Yuan Ze Fuel Cell Center, Department of Mechanical Engineering, Yuan Ze University, No. 135, Yuan-Tung Road, Chungli, Taoyuan 320, Taiwan*

Received 6 December 2010; received in revised form 17 April 2011; accepted 20 April 2011
Available online 31 May 2011

Abstract

This study reports the successful preparation of single-phase perovskite $(Ba_{0.5}Sr_{0.5})_{0.8}La_{0.2}Fe_{1-x}Mn_xO_{3-\delta}$ ($x = 0$–0.2) by the citrate–EDTA complexing method. The crystal structure, thermal gravity analysis, coefficient of thermal expansion, electrical conductivity, and electrochemical performance of $(Ba_{0.5}Sr_{0.5})_{0.8}La_{0.2}Fe_{1-x}Mn_xO_{3-\delta}$ were investigated to determine its suitability as a cathode material for intermediate-temperature solid oxide fuel cells (IT-SOFCs). The lattice parameter a of $(Ba_{0.5}Sr_{0.5})_{0.8}La_{0.2}Fe_{1-x}Mn_xO_{3-\delta}$ decreases as the amount of Mn doping increases. The coefficients of thermal expansion of the samples are in the range of 21.6–25.9 $\times 10^{-6}\,K^{-1}$ and show an abnormal expansion at around 400 °C associated with the loss of lattice oxygen. The electrical conductivity of the $(Ba_{0.5}Sr_{0.5})_{0.8}La_{0.2}Fe_{1-x}Mn_xO_{3-\delta}$ samples decreases as the amount of Mn-doping increases. The electrical conductivity of the samples reaches a maximum value at around 400 °C and then decreases as the temperature increases. The charge transfer resistance, diffusion resistance and total resistance of a $(Ba_{0.5}Sr_{0.5})_{0.8}La_{0.2}Fe_{0.8}Mn_{0.15}O_{3-\delta}$–$Ce_{0.8}Sm_{0.2}O_{1.9}$ composite cathode electrode at 800 °C are 0.11 $\Omega\,cm^2$, 0.24 $\Omega\,cm^2$ and 0.35 $\Omega\,cm^2$, respectively.

Keywords: Perovskites; Electrical properties; Impedance; Defects; Precursors-organic

1. Introduction

Solid oxide fuel cells (SOFCs) efficiently convert chemical energy into electricity in a silent and environmentally friendly manner. The SOFCs have many advantages, such as high power density, low pollution and fuel flexibility when using hydrocarbon fuels.[1–3] However, the high operating temperatures of SOFCs result in poisoning of the cathode by chromium species from Cr-based metallic interconnector and material compatibility between the electrolyte, electrode and interconnector is a challenge.[4] However, as the operating temperature of SOFCs decreases to an intermediate temperature range of 600–800 °C, the activation polarization of the cathode electrode clearly increases and the electrical conductivity and electrochemical performance of the cathode decrease. Therefore, it is important to develop a new high performance cathode material with low active polarization for intermediate-temperature SOFCs (IT-SOFCs).

Cobalt or iron-based perovskite cathode materials are known to exhibit higher ionic and electronic conductivities than other kinds of cathode materials, but they also have many disadvantages, such as a high coefficient of thermal expansion (CTE), the high cost of cobalt, and the easy evaporation and reduction of cobalt, which must be resolved.[5–8] The CTE of the cobalt-based ($\sim 20 \times 10^{-6}\,K^{-1}$) cathodes is much higher than that of the manganese-based cathode materials ($\sim 11 \times 10^{-6}\,K^{-1}$) due to the formation of oxygen vacancies, spin-state transitions associated with Co^{3+}, and the relatively weaker Co–O bond as compared with the Mn–O bond.[9–11] Iron-based perovskite cathodes have the advantage of electron or hole mobility and a low thermal expansion coefficient. Zhao reported a high power density SOFC of 718 mW/cm^2

* Corresponding author. Tel.: +886 3 4638800x2569; fax: +886 3 4630634.
E-mail address: imhung@saturn.yzu.edu.tw (I.-M. Hung).

0955-2219/$ – see front matter © 2011 Elsevier Ltd. All rights reserved.
doi:10.1016/j.jeurceramsoc.2011.04.029

using $Ba_{0.5}Sr_{0.5}Fe_{0.8}Cu_{0.2}O_{3-\delta}$ as cathode electrode. The conductivity of $Ba_{0.5}Sr_{0.5}Fe_{0.8}Cu_{0.2}O_{3-\delta}$ is 57 S/cm at 600 °C.[12] Therefore, iron-based perovskite materials may be a good candidate cathode for IT-SOFCs.

Recently, the citrate–EDTA complexing method had been widely used to prepare the SOFC cathode materials, such as $Ba_{0.5}Sr_{0.5}Co_{0.8}Fe_{0.2}O_{3-\delta}$ (BSCF), $Ba_{0.6}Sr_{0.4}Co_{0.9}Nb_{0.1}O_{3-\delta}$ and $La_{0.6}Sr_{0.5}Co_{0.2}Fe_{0.8}O_{3-\delta}$ (LSCF).[13–16,18,19,21] The cathode powder prepared from citrate–EDTA complexing method exhibits many advantages such as homogeneous element distribution, high specific surface area, nano-crystallite and low temperature synthesis, therefore, a cathode made by this method can have better electrochemical properties. In this study, $(Ba_{0.5}Sr_{0.5})_{0.8}La_{0.2}Fe_{1-x}Mn_xO_{3-\delta}$ ($x = 0.0$–0.20) was prepared by a citrate–EDTA complexing method, which enabled the formation of single-phase perovskite oxide. The crystal structure, lattice oxygen loss, coefficient of thermal expansion, electrical conductivity, and electrochemical performance of samples were investigated in detail.

2. Experiment

$(Ba_{0.5}Sr_{0.5})_{0.8}La_{0.2}Fe_{1-x}Mn_xO_{3-\delta}$ (BSLFMn) powders were prepared using the citrate–EDTA complexing method.[13–15] First, ethylenediaminetetraacetic acid (EDTA, Riedel-dehaen, 98%) was mixed with 6 M NH_4OH to form an NH_3–EDTA solution. Then, $Ba(NO_3)_2$ (J.T. Baker, 99.6%) and $La(NO_3)_3{\cdot}6H_2O$ (Alfa Aesar, 99.0%) were added, and the mixture was heated and stirred. $Sr(NO_3)_2$ (Alfa Aesar, 99.0%), $Mn(NO_3)_2{\cdot}4H_2O$ (Fluka, 99.0%) and $Fe(NO_3)_2{\cdot}6H_2O$ (J.T. Baker, 99.8%) were dissolved in another 6M NH_4OH solution. These two solutions were mixed and stirred before citric acid was added. The resulting molar ratio of EDTA:citric acid:total metal ions was 1:1.5:1. The pH was adjusted to 6 by adding a further 6 M of NH_4OH solution. The final solution was heated to 100 °C on a hotplate and stirred until water evaporated from it, leaving behind a sticky gel. This gel was then further heated at 200 °C for 3 h, calcined at 950 °C for 9 h, and sintered at 1050 °C for 5 h. The samples with different Fe/Mn ratios were designated as BSLFMn00, BSLFMn05, BSLFMn10, BSLFMn15 and BSLFMn20.

The structure of the $(Ba_{0.5}Sr_{0.5})_{0.8}La_{0.2}Fe_{1-x}Mn_xO_{3-\delta}$ powders was determined using a powder diffractometer (LabX, XRD-6000) with Ni-filtered Cu Kα radiation and a diffraction angle scanning from 20° to 85° with a step of 0.01° and a rate of 1° min^{-1}. The electrical conductivity was measured in air using a DC four-terminal method using Agilent Technologies 34970A and 6645A data acquisition/switch units with silver as the metal electrode and wire. Thermogravimetry analysis (TGA) was performed between 30 °C and 1000 °C at a heating rate of 5 °C/min in N_2, air and O_2 using TA Instruments SDT-Q600 DSC-TGA. The coefficient of thermal expansion (CTE) was measured between 50 °C and 1000 °C using a Seiko Instruments TMA/SS 6100 dilatometer with a heating rate of 5 °C/min in air. BSLFMn–30 wt% $Ce_{0.8}Sm_{0.2}O_{1.9}$ (SDC, Gimat) composite electrodes were screen printed on both sides of SDC disks to prepare symmetry cells for electrochemical impedance spectroscopy (EIS). The SDC substrate disks, 10 mm in diameter and 0.5 mm in thickness, were prepared by solid-state sintering at 1600 °C for 4 h. A slurry with proper viscosity for screen printing was typically obtained by ball-milling a mixture of 0.3 g BSLFMn ($x = 0.0$–0.20) with 0.13 g SDC powder and ethyl cellulose–terpineol (J.T. Baker) binder.[14] After screen printing, the cells were baked at 120 °C and then sintered at 1050 °C for 5 h. The EIS was measured using an impedance analyzer (HIOKI, 3532-50) at 30 mV, operating at frequencies ranging from 0.01 Hz to 1 MHz at temperatures ranging from 600–800 °C.

3. Results and discussion

Fig. 1(a) shows the XRD patterns of the BSLFMn samples sintered at 1050 °C for 5 h. All the samples were found to have an ABO_3 cubic perovskite type structure. The XRD peaks of all samples fitted well with the standard peaks of $BaFeO_{3-\delta}$ (JCPDS 75-0426). The peaks were found to gradually shift toward the high-angle direction but no other second phases were detected as the amount of Mn-doping increased. The lattice parameter a and unit cell volumes of the BSLFMn samples are shown in Fig. 1(b). The lattice parameter a of $(Ba_{0.5}Sr_{0.5})_{0.8}La_{0.2}Fe_{1-x}Mn_xO_{3-\delta}$ decreased from 3.912 Å to 3.895 Å and the cell volume decrease from 59.79 $Å^3$ to 59.09 $Å^3$

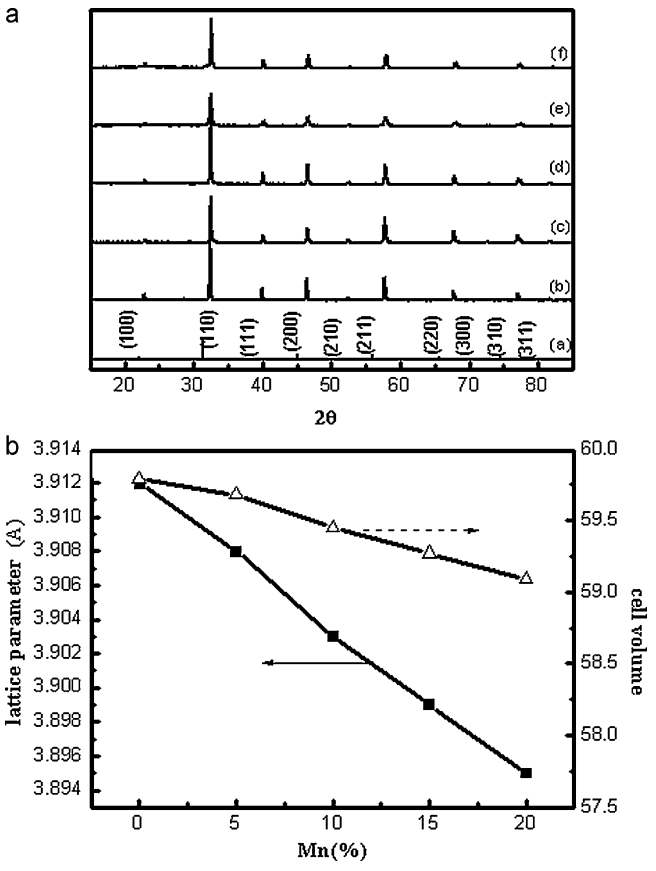

Fig. 1. (A) XRD patterns of $(Ba_{0.5}Sr_{0.5})_{0.8}La_{0.2}Fe_{1-x}Mn_xO_{3-\delta}$. (a) $BaFeO_3$ JCPDF 75-0426, (b) $x = 0.00$, (c) $x = 0.05$, (d) $x = 0.10$, (e) $x = 0.15$ and (f) $x = 0.20$. (B) Lattice parameter and cell volume of $(Ba_{0.5}Sr_{0.5})_{0.8}La_{0.2}Fe_{1-x}Mn_xO_{3-\delta}$ depends on x.

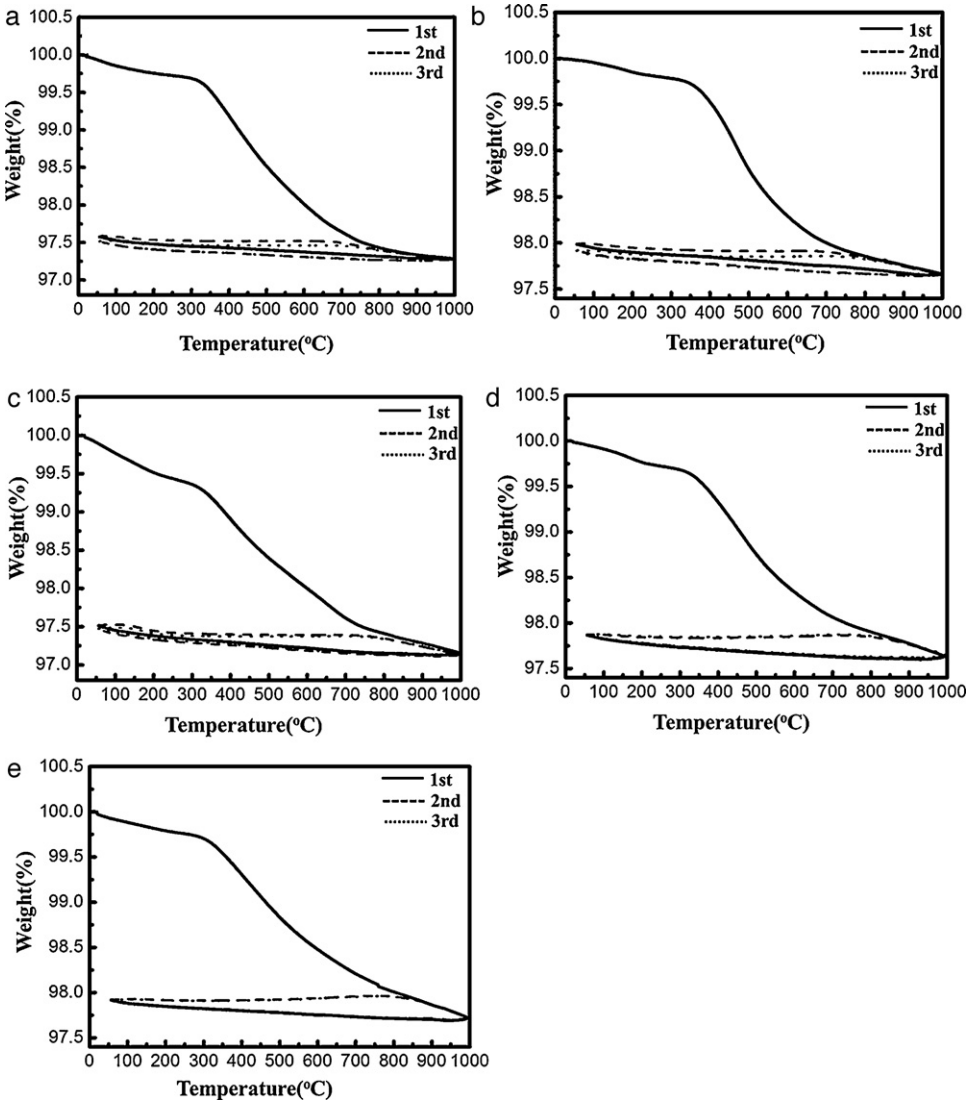

Fig. 2. Thermogravimetry analysis (TGA) plots of $(Ba_{0.5}Sr_{0.5})_{0.8}La_{0.2}Fe_{1-x}Mn_xO_{3-\delta}$. (a) $x = 0.00$, (b) $x = 0.05$, (c) $x = 0.10$, (d) $x = 0.15$, (e) $x = 0.20$.

as the amount of Mn-doping increased from 0 to 20 mol%. The lattice parameter and cell volume of samples decreased as the amount of Mn^{4+} substituting for Fe^{4+} increased because the ion radius of Mn^{4+} (0.53 Å) is much smaller than that of the Fe^{4+} (0.585 Å).

Fig. 2 shows thermogravimetric analysis (TGA) curves of samples measured in a three cycle process in N_2. The mass loss of TGA values is due to oxygen loss indicating the formation of oxygen vacancies. From room temperature to 300 °C, the weight reduced slightly due to the evaporation of water adsorbed on the surface of the samples.[16] As the temperature increased from 300 to 1000 °C, the mass of the sample obviously decreased as the temperature increased due to the loss of oxygen and the formation of oxygen vacancies. The mass loss decreased from 2.403% to 1.985% for samples as the amount of Mn-doping increased to 20 mol% in the temperature range of 300–1000 °C. The concentration of oxygen vacancies in the samples affected the charge resistance that was measured by the AC impedance, as discussed in more detail later. After the three heating and cooling cycles, the mass loss of the samples showed good reproducibility, indicating that all samples captured and released oxygen according to the temperature.[17] In order to identify the weight of samples is due to loss of oxygen in lattice, the TGA of BSLFMn0 and BSLFMn15 samples were conducted in N_2, air and O_2 atmospheres as shown in Table 1. Comparing the mass loss and increase of samples during the heating and cooling process in 3 cycles, it was found that the mass loss during heating are similar with the weight increase during cooling in O_2 and air atmospheres for BSLFMn0 and BSLFMn15 samples. However, the mass loss of samples during heating are much larger than the weight increase during cooling in N_2 atmosphere because the oxygen partial pressure in N_2 atmosphere is much lower than that in O_2 and air atmospheres. Therefore, only a little amount of oxygen is resumed to the lattice during cooling process in N_2 atmosphere.

The thermal expansion curves and values of the BSLFMn samples are shown in Fig. 3 and Table 2, respectively. The thermal expansion curve of the BSLFMn samples was linear

Table 1
The oxygen mass loss (%) and increase of BSLFMn0 and BSLFMn15 in N_2, air and O_2 in 3 cycles.

Cycle		Sample					
		BSLFMn0			BSLFMn15		
		N_2	Air	O_2	N_2	Air	O_2
1st	300–1000 °C (heating)	−1.90	−1.85	−1.78	−1.63	−1.59	−1.35
	1000–200 °C (cooling)	0.02	1.82	1.78	0.23	1.25	1.33
2nd	300–1000 °C (heating)	−0.09	−1.83	−1.83	−0.27	−1.45	−1.37
	1000 –200 °C (cooling)	0.03	1.82	1.83	0.15	1.45	1.33
3rd	300–1000 °C (heating)	−0.09	−1.84	−1.80	−0.22	−1.44	−1.38
	1000–200 °C (cooling)	0.04	1.80	1.78	0.12	1.45	1.36

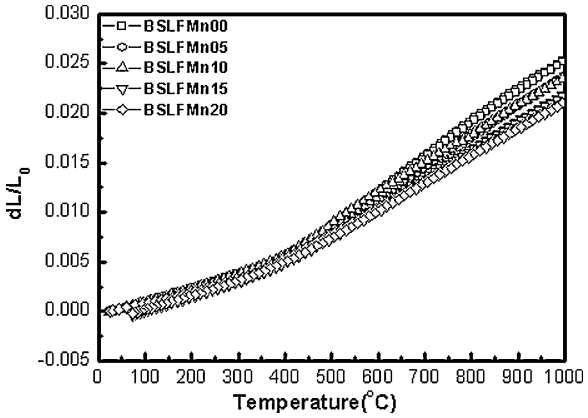

Fig. 3. Thermal expansion curves of $(Ba_{0.5}Sr_{0.5})_{0.8}La_{0.2}Fe_{1-x}Mn_xO_{3-\delta}$ from room temperatures to 1000 °C.

in the low temperature range of 50–400 °C, with a low CTE of 14.7–15.5 × 10^{-6} K^{-1}. A significant inflection occurs above 400 °C, with a high CTE of 26.4–33 × 10^{-6} K^{-1} between 400 °C and 1000 °C, due to the loss of the lattice oxygen and the formation of oxygen vacancies followed by the reduction of Mn^{4+} to Mn^{3+} or Fe^{3+} to Fe^{2+}. Obviously, the CTE of the BSLFMn samples decreased as amount of Mn doping increased from 25.9 × 10^{-6} K^{-1} (x = 0.0) to 21.6 × 10^{-6} K^{-1} (x = 0.2). The reduction of the B-site cations to the lower states is expected to occur to maintain electrical neutrality, according to Eq. (1):

$$2B_B^X + O_O^X \leftrightarrow 2B_B' + V_O^{\bullet\bullet} + \frac{1}{2}O_2 \quad (1)$$

The reduction of Fe^{4+} (0.585 Å)/Mn^{4+} (0.53 Å) is associated with an increase in the Fe^{3+} (0.645 Å)/Mn^{3+} (0.645 Å) ionic radius; therefore, thermal expansion values of the BSLFMn samples increased as the temperature increased. According to Pauling's second rule, the reduction of B^{4+} to B^{3+} is associated with an increase in the B-site ionic radius, resulting in a decrease in the B–O bond enhancing the lattice thermal expansion.[18,19]

An ideal cathode material should exhibit two conductive mechanisms, which include the electronic and ionic conductivity for IT-SOFCs. Fig. 4(a) shows the electrical conductivity of the BSLFMn samples as a function of temperature. The electrical conductivity of all samples was found to increase to a maximum at around 400 °C and then decreased as the temperature increased further. The formation of oxygen vacancies at high temperatures results in a reduction of B site cations and an increase in the concentration of electron holes.

Table 2
Coefficient of thermal expansion (CTE) of $(Ba_{0.5}Sr_{0.5})_{0.8}La_{0.2}Fe_{1-x}Mn_xO_{3-\delta}$ electrodes.

x value	50–400 °C (x 10^{-6} K^{-1})	400–1000 °C (x 10^{-6} K^{-1})	25–1000 °C (x 10^{-6} K^{-1})
0	15.5	33.0	25.9
5	14.8	30.8	24.3
10	15.3	30.1	24.0
15	14.7	27.7	22.4
20	14.7	26.4	21.6

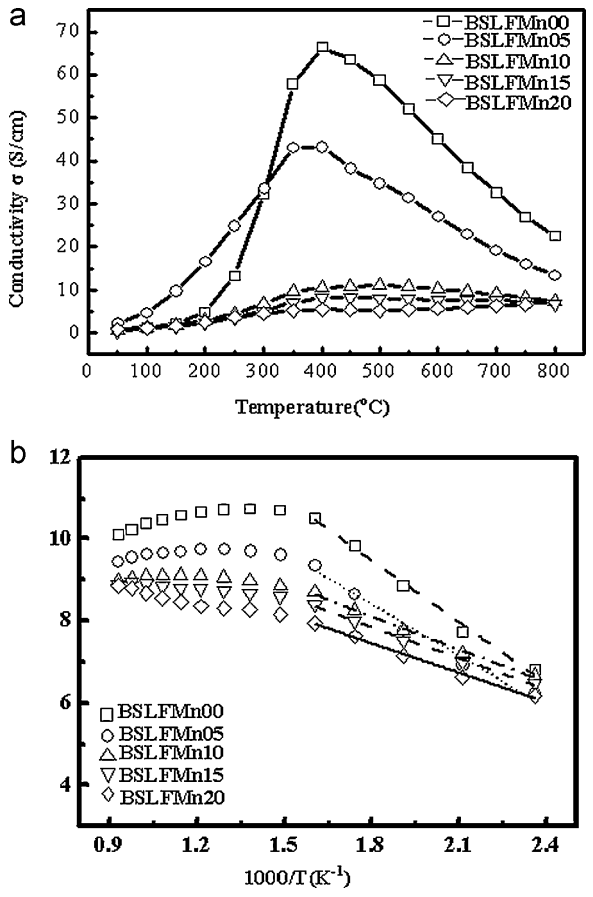

Fig. 4. (a) Conductivity of $(Ba_{0.5}Sr_{0.5})_{0.8}La_{0.2}Fe_{1-x}Mn_xO_{3-\delta}$ and (b) Arrhenius plot of conductivity of $(Ba_{0.5}Sr_{0.5})_{0.8}La_{0.2}Fe_{1-x}Mn_xO_{3-\delta}$ with different x values.

Table 3
The activation energy of conductivity of $(Ba_{0.5}Sr_{0.5})_{0.8}La_{0.2}Fe_{1-x}Mn_xO_{3-\delta}$.

x value	E_a (kJ/mol)
0	41.63
5	34.08
10	21.75
15	20.85
20	18.95

The maximum conductivity of $(Ba_{0.5}Sr_{0.5})_{0.8}La_{0.2}FeO_{3-\delta}$ is 67 S/cm at 400 °C, and decreased to 7 S/cm as the amount of Mn doping increased to 20 mol%. Even the electrical conductivity of the BSLFMn samples is not as high as that of the other cathode materials; however, a high power density of SOFC was reported using $Ba_{0.5}Sr_{0.5}Co_{0.8}Fe_{0.2}O_{3-\delta}$ (BSCF) as the cathode. It is well known that the maximum conductivity of $Ba_{0.5}Sr_{0.5}Co_{0.8}Fe_{0.2}O_{3-\delta}$ (BSCF) is only about 45 S/cm, but it displays a good electrochemical performance for oxygen reduction.[20] The conductivity mechanism of perovskite-type oxides depends on Zerner double exchange.[21] Fig. 4(b) shows the Arrhenius plots of the conductivity of $(Ba_{0.5}Sr_{0.5})_{0.8}La_{0.2}Fe_{1-x}Mn_xO_{3-\delta}$, which is described by the following equation:

$$\sigma = \frac{A}{T}\exp\left(-\frac{E_a}{KT}\right) \quad (2)$$

where E_a is the activation energy, T is the temperature in Kelvin, k is Boltzmann's constant, and A is the pre-exponential factor. The calculated activation energy (E_a) values are listed in Table 3. The activation energy of the samples decreased from 41.63 kJ/mol to 18.95 kJ/mol as the amount of Mn-doping increased to 20 mol%. The activation energy of the BSLFMn samples is a little higher than that of $(Ba_{0.5}Sr_{0.5})_{0.8}La_{0.2}CoO_{3-\delta}$.[14] The activation energy of the BSLFMn samples decreased with an increase in the Mn content may be due to the bandwidth decreased and the polaron binding energy increased.[22]

The resistance data of the BSLFMn–SDC composite electrodes fitted using the equivalent circuit and measured at 600–800 °C in air correspond to electrochemical processes.[15,23,24] R1 includes the electrolyte, electrode and lead ohmic resistance; R2 corresponds to the resistance of the charge transfer process. R3 corresponds to the adsorption–desorption of oxygen, oxygen diffusion at the gas–cathode interface, and the surface diffusion of intermediate oxygen species. Fig. 5 shows R2, R3 and area specific resistance (ASR)[25] at various temperatures and the values are listed in Table 4. It was found that the R2 of BSLFMn0–30%SDC was much smaller than that of the other samples, because of the high vacancy concentration of the BSLFMn0 sample, which led to faster oxygen ion transport and surface exchange, and this was supported by the TGA result.[26] However, R3 of BSLFMn0–30%SDC was much higher than that of the other samples, which was due to the low gas diffusion on the surface of the BSLFMn0 sample. Fig. 6 shows the microstructure of the BSLFMn composite electrodes sintered at 1050 °C for 5 h. The grain size of BSLFMn0 is about

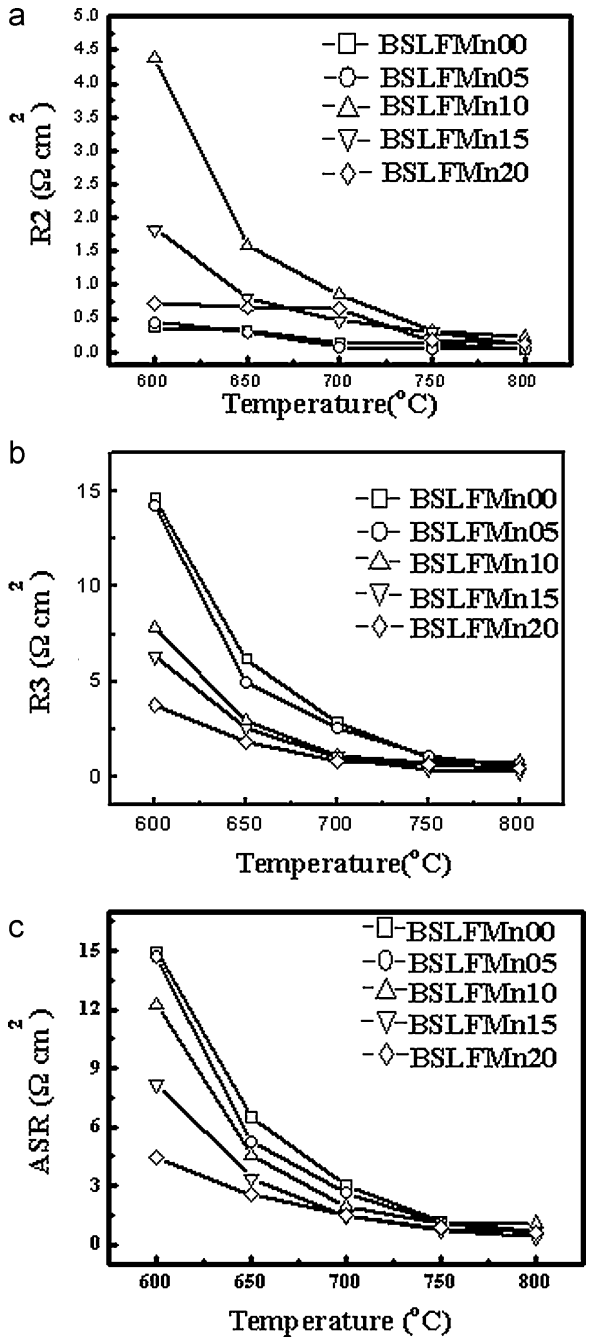

Fig. 5. (a) Charge-transfer resistance, (b) oxygen ion diffusion and (c) total resistance of $(Ba_{0.5}Sr_{0.5})_{0.8}La_{0.2}Fe_{1-x}Mn_xO_{3-\delta}$ with different x values.

3–5 μm, which is much higher than that of the other samples (about 1 μm); therefore, the gas diffusion pathway on the surface of BSLFMn0 is lower than that of the other samples. Comparing the total resistance of all samples, shown in Fig. 5(c), the BSLFMn15 sample was found to have a lower resistance than the other samples at 700–800 °C. The material with 15% Mn shows a potential candidate as a cathode material for IT-SOFC.

The conductivity of BSLFMn0 and BSLFMn15 samples at 600 °C in air for 100 h is shown Fig. 7. The conductivity of BSLFMn0 and BSLFMn15 respectively was 40.8 S/cm and 16.2 S/cm at 600 °C for 100 h. The conductivity of these two samples did not significantly decrease after long time testing.

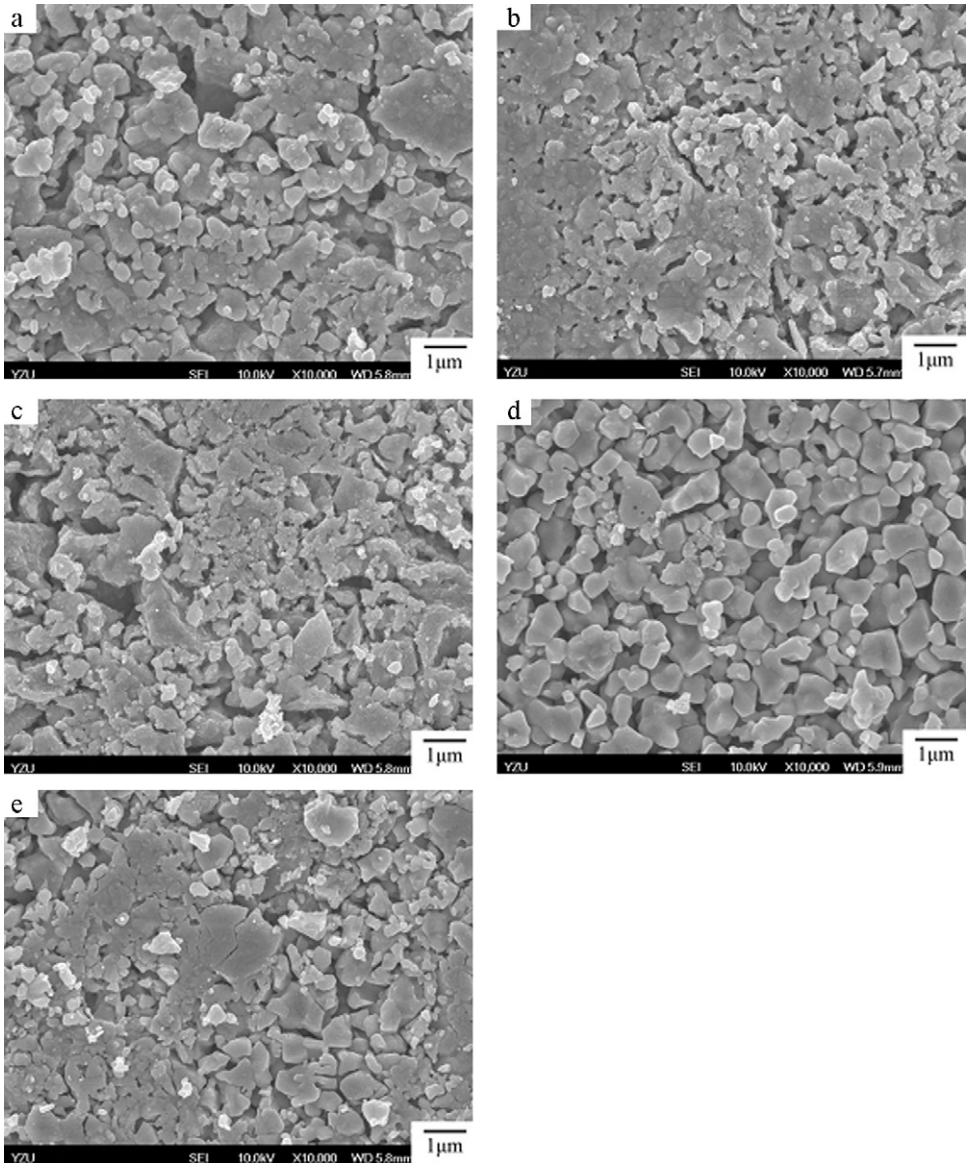

Fig. 6. SEM micrographs of $(Ba_{0.5}Sr_{0.5})_{0.8}La_{0.2}Fe_{1-x}Mn_xO_{3-\delta}$ sintered at 1050 °C for 5 h. (a) $x = 0.00$, (b) $x = 0.05$, (c) $x = 0.10$, (d) $x = 0.15$, (e) $x = 0.20$.

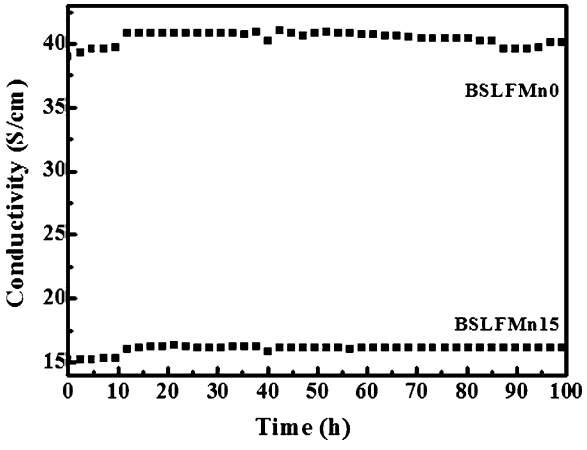

Fig. 7. The conductivity of $(Ba_{0.5}Sr_{0.5})_{0.8}La_{0.2}Fe_{1.0}Mn_0O_{3-\delta}$ and $(Ba_{0.5}Sr_{0.5})_{0.8}La_{0.2}Fe_{0.85}Mn_{0.15}O_{3-\delta}$ at 600 °C for 100 h.

Table 4
Resistance values ($\Omega\,cm^2$) of $(Ba_{0.5}Sr_{0.5})_{0.8}La_{0.2}Fe_{1-x}Mn_xO_{3-\delta}$ at different temperatures.

x value		°C				
		600	650	700	750	800
Mn0	R2	0.37	0.32	0.14	0.12	0.03
	R3	14.61	6.20	2.87	1.02	0.62
	ASR	14.98	6.52	3.01	1.14	0.65
Mn05	R2	0.44	0.29	0.07	0.05	0.04
	R3	14.24	4.95	2.57	1.08	0.46
	ASR	14.68	5.24	2.64	1.13	0.5
Mn10	R2	4.38	1.58	0.85	0.30	0.23
	R3	7.83	2.94	1.06	0.70	0.82
	ASR	12.21	4.52	1.91	1.00	1.05
Mn15	R2	1.83	0.80	0.42	0.30	0.11
	R3	6.32	2.59	1.01	0.37	0.24
	ASR	8.15	3.39	1.43	0.67	0.35
Mn20	R2	0.73	0.66	0.64	0.17	0.12
	R3	3.73	1.88	0.86	0.66	0.51
	ASR	4.46	2.54	1.5	0.83	0.63

4. Conclusion

$Ba_{0.4}Sr_{0.4}La_{0.2}Fe_{1-x}Mn_xO_{3-\delta}$ ($x = 0$–0.2) cathode materials with cubic perovskite structure were successfully prepared by the citrate–EDTA complexing method. The lattice constant of $Ba_{0.4}Sr_{0.4}La_{0.2}Fe_{1-x}Mn_xO_{3-\delta}$ clearly decreased as the amount of Mn-doping increased. The thermal expansion and thermogravimetry analysis curves show abnormal expansion at around 400 °C, which was attributed to the loss of lattice oxygen. AC impedance measurements reveal a low resistance of 0.35 $\Omega\,cm^2$ for a $(Ba_{0.5}Sr_{0.5})_{0.8}La_{0.2}Fe_{0.8}Mn_{0.15}O_{3-\delta}$–30 wt% $Ce_{0.8}Sm_{0.2}O_{1.9}$ composite electrode at 800 °C.

Acknowledgements

The authors acknowledge the financial support from the National Science Council in Taiwan under contract No. NSC 100-3113-E-155-001 and NSC 100-3113-E-006-011. The authors thank Prof. Kuan-Zong Fung (Department of Materials Science and Engineering, National Cheng Kung University) and Prof. Wen-Cheng Wei (Department of Materials Science and Engineering, National Taiwan University) for their kind advices.

References

1. Minh NQ. Ceramic fuel cells. *Journal of the American Ceramic Society* 1993;**76**:563–88.
2. Goodenough JB, Huang YH. Alternative anode materials for solid oxide fuel cells. *Journal of Power Sources* 2007;**173**:1–10.
3. Zhou W, Ran R, Shao ZP. Progress in understanding and development of $Ba_{0.5}Sr_{0.5}Co_{0.8}Fe_{0.2}O_{3-\delta}$-based cathodes for intermediate-temperature solid-oxide fuel cells: a review. *Journal of Power Sources* 2009;**192**:231–346.
4. Jiang SP, Zhang JP, Zheng XG. A comparative investigation of chromium deposition at air electrodes of solid oxide fuel cells. *Journal of the European Ceramic Society* 2002;**22**:361–73.
5. Tai LW, Nasrallah MM, Anderson HU, Sparlin DM, Sehlin SR. Structure and electrical properties of $La_{1-x}Sr_xCo_{1-y}Fe_yO_3$. Part 1. The system $La_{0.8}Sr_{0.2}Co_{1-y}FeyO_{3-\delta}$. *Solid State Ionics* 1995;**76**:259–71.
6. Yasumoto K, Inagaki Y, Shiono M, Dokiya M. An (La,Sr)(Co,Cu)$O_{3-\delta}$ cathode for reduced temperature SOFCs. *Solid State Ionics* 2002;**148**:545–9.
7. Wei B, Lu Z, Huang XQ, Liu ML, Li N, Su WH. Synthesis, electrical and electrochemical properties of $Ba_{0.5}Sr_{0.5}Zn_{0.2}Fe_{0.8}O_{3-\delta}$ perovskite oxide for IT-SOFC cathode. *Journal of Power Sources* 2008;**176**:1–8.
8. Ling Y, Zhao L, Lin B, Dong YC, Zhang XZ, Meng GY, et al. Investigation of cobalt-free cathode material $Sm_{0.5}Sr_{0.5}Fe_{0.8}Cu_{0.2}O_{3-\delta}$ for intermediate temperature solid oxide fuel cell. *International Journal of Hydrogen Energy* 2010;**35**:6905–10.
9. Lee KT, Manthiram A. Comparison of $Ln_{0.6}Sr_{0.4}CoO_{3-\delta}$ (Ln = La, Pr, Nd, Sm, and Gd) as cathode materials for intermediate temperature solid oxide fuel cells. *Journal of the Electrochemical Society* 2006;**153**:A794–798.
10. Huang K, Lee HY, Goodenough JB. Sr- and Ni-doped $LaCoO_3$ and $LaFeO_3$ perovskites. *Journal of the Electrochemical Society* 1998;**145**:3220–7.
11. Weber A, Tiffée EI. Materials and concepts for solid oxide fuel cells (SOFCs) in stationary and mobile applications. *Journal of Power Sources* 2004;**127**:273–83.
12. Zhao L, He B, Zhang XZ, Peng RR, Meng GY, Liu XQ. Electrochemical performance of novel cobalt-free oxide $Ba_{0.5}Sr_{0.5}Fe_{0.8}Cu_{0.2}O_{3-\delta}$ for solid oxide fuel cell cathode. *Journal of Power Sources* 2010;**195**:1859–61.
13. Liu Z, Han MF, Miao WT. Preparation and characterization of graded cathode $La_{0.6}Sr_{0.4}Co_{0.2}Fe_{0.8}O_{3-\delta}$. *Journal of Power Sources* 2007;**173**:837–41.
14. Hung IM, Liang CY, Ciou CJ, Lee YC. Conductivity and electrochemical performance of $(Ba_{0.5}Sr_{0.5})_{0.8}La_{0.2}CoO_{3-\delta}$cathode for intermediate-temperature solid oxide fuel cell. *Ceramics International* 2010;**36**:1937–43.
15. Wang K, Ran R, Zhou W, Gu HX, Shao ZP, Ahn JM. Properties and performance of $Ba_{0.5}Sr_{0.5}Co_{0.8}Fe_{0.2} + Sm_{0.2}Ce_{0.8}O_{1.9}$ composite cathode. *Journal of Power Sources* 2008;**179**:60–8.
16. Li SY, Lü Z, Huang XQ, Wei B, Su WH. Thermal, electrical, and electrochemical properties of lanthanum-doped $Ba_{0.5}Sr_{0.5}Co_{0.8}Fe_{0.2}O_{3-\delta}$. *Journal of Physics and Chemistry of Solids* 2007;**68**:1707–12.
17. Ovenstone J, Jung JL, White JS, Edwards DD, Misture ST. Phase stability of BSCF in low oxygen partial pressures. *Journal of Solid State Chemistry* 2008;**181**:576–86.
18. Wei B, Lu Z, Huang XQ, Miao JP, Sha XQ, Xin XS, et al. Crystal structure, thermal expansion and electrical conductivity of perovskite oxides $Ba_xSr_{1-x}Co_{0.8}Fe_{0.2}O_{3-\delta}$ ($0.3 \le x \le 0.7$). *Journal of the European Ceramic Society* 2006;**26**:2827–32.
19. Wei B, Lu Z, Li SY, Liu YQ, Liu KY, Su WH. Thermal and electrical properties of new cathode material $Ba_{0.5}Sr_{0.5}Co_{0.8}Fe_{0.2}O_{3-\delta}$ for solid oxide fuel cells. *Electrochemical and Solid-State Letters* 2005;**8**:A428–31.
20. Shao ZP, Haile SM. A high performance cathode for the next generation of solid oxide fuel cells. *Nature* 2004;**431**:170–3.
21. Huang C, Chen DJ, Lin Y, Ran R, Shao ZP. Evaluation of $Ba_{0.6}Sr_{0.4}Co_{0.9}Nb_{0.1}O_{3-\delta}$ mixed conductor as a cathode for intermediate-temperature oxygen-ionic solid-oxide fuel cells. *Journal of Power Sources* 2010;**195**:5176–84.
22. Ding XF, Cui C, Du XJ, Guo LC. Electrical conductivity, thermal expansion and electrochemical properties of Fe-doped $La_{0.7}Sr_{0.3}CuO_{3-\delta}$ cathodes for solid oxide fuel cells. *Journal of Alloys and Compounds* 2009;**475**: 418–21.
23. Zhou W, Jin WQ, Zhu ZG, Shao ZP. Structural, electrical and electrochemical characterizations of $SrNb_{0.1}Co_{0.9}O_{3-\delta}$ as a cathode of solid oxide fuel cells operating below 600 °C. *International Journal of Hydrogen energy* 2010;**35**:1356–66.
24. Vladikova DE, Stoynov ZB, Barbucci A, Viviani M, Carpanese P, Kilner JA, et al. Impedance studies of cathode/electrolyte behaviour in SOFC. *Electrochimica Acta* 2008;**53**:7491–9.
25. Lee CG, Bae JG. Effect of effective areas on ionic conductivity in dense composite material composed of ionic and electronic conductors for solid oxide fuel cells. *Solid State Ionics* 2008;**179**:2031–6.
26. Liu BW, Zhang Y, Zhang LM. Oxygen reduction mechanism at $Ba_{0.5}Sr_{0.5}Co_{0.8}Fe_{0.2}O_{3-\delta}$ cathode for solid oxide fuel cell. *International Journal of Hydrogen energy* 2009;**34**:1008–14.